

INFRA-RED SIGNATURE OF WARSHIPS

BY

P. J. GATES, PH.D., C.ENG., M.I.E.E., R.C.N.C.
(on secondment to CAP (Scientific) Ltd.)

ABSTRACT

There are two atmospheric transmission bands through which the IR signature of a warship may be detected. In general, emissions in the MIR band (3–5 μm) are produced by very hot objects and are exploited by homing missiles, whereas the FIR band (8–14 μm) has a signature which is produced by objects closer to ambient temperature. This has found more use for covert target identification.

Ship signatures can be reduced and modified to make their exploitation more difficult, especially where background conditions are complicated. These measures will never be wholly effective but will greatly enhance the effectiveness of decoys and increase the survivability of the high value units to which they are fitted.

Introduction

All materials emit radiation in the infra-red (IR) region of the electromagnetic spectrum. This IR energy can be used to detect the presence of warships, providing missiles with a means of homing on to their target. In this article the factors affecting IR emissions are outlined. Methods of reducing and modifying them in order to reduce the ship's detectability are also discussed.

To begin, it is worthwhile considering the differences between the detection of ships by IR emission and radar, which remains the principal means of ship detection. The first difference is that IR detection is passive, identifying emitted energy, whereas radar is an active technique beaming energy at the target and detecting that which is reflected. Passive detection provides only bearing information and cannot give the target range as a pulsed radar does. In addition, sensitivity cannot be increased by using techniques such as pulse compression or boosting the illuminating power which are available to active techniques. Indeed the small amounts of IR energy emitted coupled with the low sensitivity of current IR detectors and poor propagation properties of the atmosphere make IR techniques unattractive for the detection of warships at ranges greater than about 10 km.

IR detection has found a potent use, however, in missile homing heads for two reasons. The first is that, being a passive technique, it is covert and it does not announce its presence (as a radar homing head alerts the Electronic Surveillance Measures equipment). Secondly, it is not susceptible to jamming techniques used against active detectors. Indeed the success of radar counter-measures has made the design of suitable radar homing heads more difficult. The spread of shipborne equipment to decoy, jam and confuse missile radars has reduced their effectiveness. To regain this performance would mean missile radars of increased sophistication which would use weight and space allocated to explosive and would considerably increase the cost of the weapon. The missile designers have thus turned to IR sensors, either alone or in combination with radars, to give their homing heads a greater probability of distinguishing between targets and decoys.

IR detection of ships at modest ranges does prove attractive for submarines which can be fitted with a detector for use at periscope depth. This enables the submarine to detect and identify targets covertly even in darkness and low visibility.

Passive detection of a ship depends on a number of factors:

- (a) the energy emitted towards the detector by the ship;
- (b) the propagation conditions;
- (c) the energy produced in the vicinity of the ship (background clutter).

The first of these factors, the emitted energy, is determined by the ship's infra-red signature, a term which describes the spatial and frequency distribution of the emission. Modification and reduction of this signature to reduce the probability of detection must take into account both propagation conditions and background, both of which will be discussed in this article.

In passing, it is worth mentioning that lasers working in the IR region such as the 1.06 μm neodymium/glass and neodymium/yttrium aluminium garnate lasers are used in active detection (range-finding) at sea over short ranges. Carbon dioxide lasers at 10.6 μm may extend this use. The signature of such reflected IR radiation is *not* the signature of emitted IR radiation which is discussed in this article and will exhibit a completely different form.

The Infra-red Spectrum

Electromagnetic waves span wavelengths from hundreds of kilometers to fractions of a nanometer (10^{-9} metre)—a range of frequencies covering more than 18 decades. Of this vast range the human eye can only detect those which lie between 0.4 μm and 0.75 μm . If this range of wavelengths is displayed, as it is in a rainbow, the eye will recognise them as gradually varying from violet (0.4 μm) through indigo, blue, green, yellow, orange to red (0.75 μm). It is the wavelengths longer than red (0.75 μm to 1 mm), undetectable to the human eye, which are termed the infra-red wavelengths (FIG. 1). The infra-red region is, for convenience, subdivided into four parts

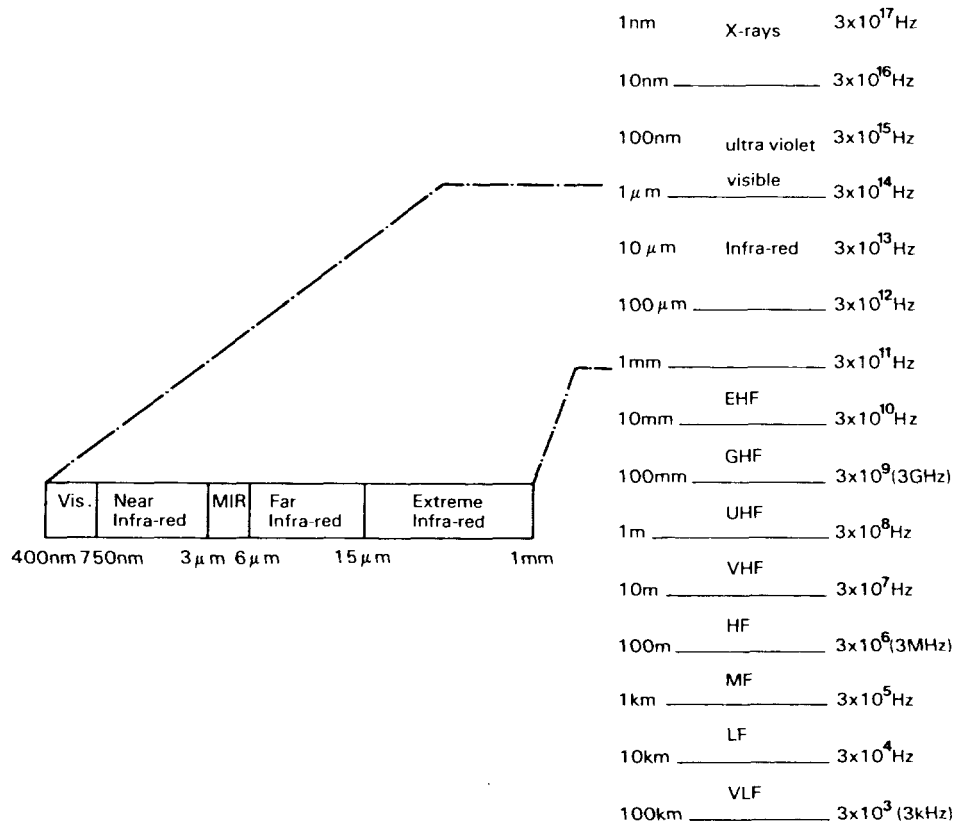


FIG. 1—THE ELECTROMAGNETIC SPECTRUM

each of which is named to indicate its proximity to the visible region, with the Near Infra-red band being closest to the visible region and the Extreme Infra-red (XIR) being furthest from it. Radar wavelengths occupy the region above 1 mm although the exact division between the XIR and radar bands is becoming blurred. The definitions of the IR bands are:

Near Infra-red (NIR): 0.75 μm (400 THz) to 3 μm (100 THz)
 Middle Infra-red (MIR): 3 μm (100 THz) to 6 μm (50 THz)
 Far Infra-red (FIR): 6 μm (50 THz) to 15 μm (20 THz)
 Extreme Infra-red (XIR): 15 μm (20 THz) to 1 mm (300 GHz)
 (Note: 1 THz = 10^{12} Hz).

The regions of particular interest in ship detection are the MIR and FIR bands, not solely because of emission characteristics but because it is these bands in which propagation conditions are most favourable.¹

Emission of Infra-red Radiation

All objects emit electromagnetic radiation in the infra-red region. Except in the case of transparent substances such as gases, this is a surface effect which depends on the nature of the surface and its temperature. The hotter the object the more energy it emits as a general rule. In addition, the median wavelength of the emissions decreases with temperature. Objects at room temperature emit most of their energy in the FIR band whereas those at temperatures of about 1000°C and above emit predominantly in the NIR band. At these temperatures there is a significant emission into the visible region as well and the objects appear to 'glow red'. Higher temperatures extend the emissions right across the visible band giving the 'white hot' appearance of very hot objects.²

The theory of infra-red emission is based upon the concept of a perfectly efficient emitter. This is termed a 'black body' because matt black objects come closest to the ideal.

The total energy per unit time (power) emitted per unit area of a black body into a hemisphere is given by the Stefan-Boltzmann law:

$$W = \frac{2 \pi^5 k^4}{15 c^2 h^3} T^4 = 5.67 \times 10^{-8} T^4 \quad (\text{J.s.}^{-1}\text{m.}^{-2} \text{ } ^\circ\text{K}^{-4})$$

where W is the radiant emittance (W.m^{-2} , $^\circ\text{K}^{-4}$) (as 1 Joule/sec = 1 Watt)

T is the absolute temperature of the body ($^\circ\text{K}$)

c is the velocity of light (approx. $3 \times 10^8 \text{ m.s}^{-1}$)

h is Planck's constant (approx. $6.63 \times 10^{-34} \text{ J.s}$)

k is Boltzmann's constant (approx. $1.38 \times 10^{-23} \text{ J.}^\circ\text{K}^{-1}$)

This power is emitted over a range of wavelengths. An equation derived by Planck shows the distribution of this power across the spectrum. Planck was able to show that this spectral distribution of radiation from a black body was related to temperature by:

$$W_\lambda \text{ d}\lambda = \frac{2\pi hc^2}{\lambda^5} \frac{\text{d}\lambda}{\exp\{ch/\lambda kT\} - 1}$$

where W_λ is the spectral radiant emittance ($\text{W.m}^{-2}.\mu\text{m}^{-1}$) emitted into a hemisphere

λ is the wavelength

This equation for the power (energy per unit time) emitted is derived from the usual equation which refers to energy emitted within a closed cavity. For the purposes of IR signatures this equation, the power emitted over a hemisphere, is more useful. Alternatively, the power emitted into unit solid angle (the

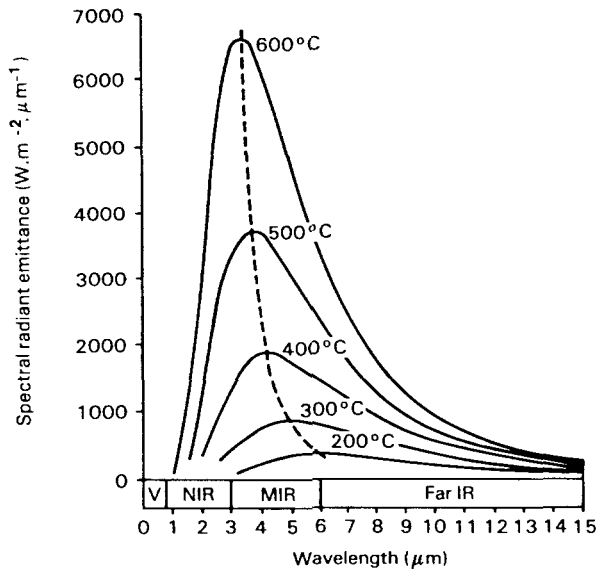


FIG. 2—SPECTRAL RADIANT EMITTANCE OF A BLACK BODY AT VARIOUS TEMPERATURES, RADIATING INTO A HEMISPHERE

angular spectral radiant emittance), may be expressed by omitting the π . The angular equation has the units $W.m^{-2}.\mu m^{-1}.sr^{-1}$. The unit of solid angle, one steradian (sr), subtends an area r^2 at a distance r .

The spectral radiant emittance is the power emitted per unit wavelength by unit area of the black body over a hemisphere. It should thus have the units $J.s^{-1}.m^{-3}$ (or the equivalent $W.m^{-3}$) but, for convenience, is usually related to $1 \mu m$ as the unit of wavelength and is thus expressed in $W.m^{-2}.\mu m^{-1}$. FIG. 2 shows the emittance for black bodies at various temperatures. As will be seen the peak emittance at about $200^\circ C$ occurs at $6 \mu m$ whereas a black body at

about $600^\circ C$ has a peak at the lower end of the MIR (at $3 \mu m$) with a twenty-fold increase in the peak emittance.

In practice few objects behave like black body radiators. Some, termed grey body radiators, have an emittance which follows the general form of a black body but with emittance reduced in magnitude. The ratio of the emittance of a radiator and that of a black body at the same temperature is termed the Spectral Emissivity. As black body radiators are perfect emitters it follows that the emissivity is always less than unity; that of a grey body will be constant as its emittance is a constant fraction of that of black body. Most objects have a more complex emissivity which depends on wavelength. These are termed selective radiators. FIG. 3(a) shows the emittance of black body, grey body and selective radiators. Their emissivity is shown in FIG. 3(b).

The emissivity of radiators depends on the nature of their surface and may also be temperature-dependent. Metals have low emissivities, especially if highly polished, which increase with temperature. Conversely, non-metals have high emissivities (above 0.8) which decrease with temperature. As emissivity is a surface property of opaque materials, they adopt the emissivity

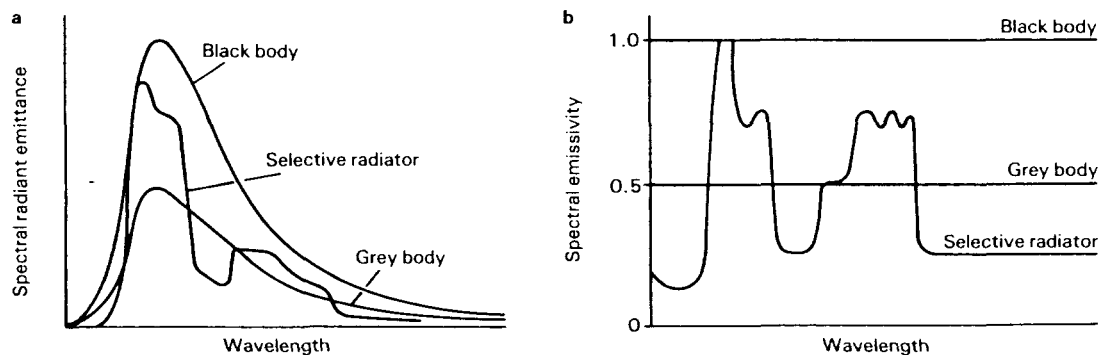


FIG. 3—(a) THE SPECTRAL RADIANT EMITTANCE, AND (b) THE SPECTRAL EMISSIVITY OF A PERFECT EMITTER (BLACK BODY RADIATOR), A GREY BODY RADIATOR, AND A SELECTIVE RADIATOR

of any paintwork or surface coating which is applied. The emissivity of these are generally very high, of the order 0.94 for oil paints and 0.99 for matt lacquer (both values apply at 100°C). Painted objects thus behave very much like black bodies over most of the infra-red spectrum.

Not only do materials emit infra-red radiation but they absorb it as well; their ability to emit and absorb being directly related by Kirchhoff's law. The wavelengths at which a material has a high emissivity are those at which it absorbs well. Conversely, where it is a poor emitter it also absorbs very little energy. An example of this selective emission and absorption occurs with both snow and clouds. These appear white because they are poor absorbers in the visible region (as they are also in the NIR). They thus reflect most incident radiation and, by Kirchhoff's law, also emit very little. In the remainder of the IR region, however, they are 'black', emitting strongly and absorbing a high proportion of the energy in these wavelengths which falls upon them.

As might be expected, neither IR emission nor absorption exhibits directional properties except for a highly polished surface. In general IR emissions are isotropic and the intensity depends only on the area visible to the detector.

Propagation Conditions

Between the emitter and any detector IR radiation is attenuated. This attenuation (sometimes referred to as extinction) follows an exponential law. This means that if its intensity falls to half its initial value after travelling a distance, d , then it will be attenuated by a further 50% in travelling a further distance d (i.e. its intensity will have fallen to 0.25 of its initial value a distance $2d$ from the source).

There are two mechanisms by which IR radiation is attenuated in the atmosphere: absorption by atmospheric gases, and scattering by small particles and water droplets. The coefficient of attenuation in the equation describing the exponential attenuation is the sum of two terms representing absorption and scattering.

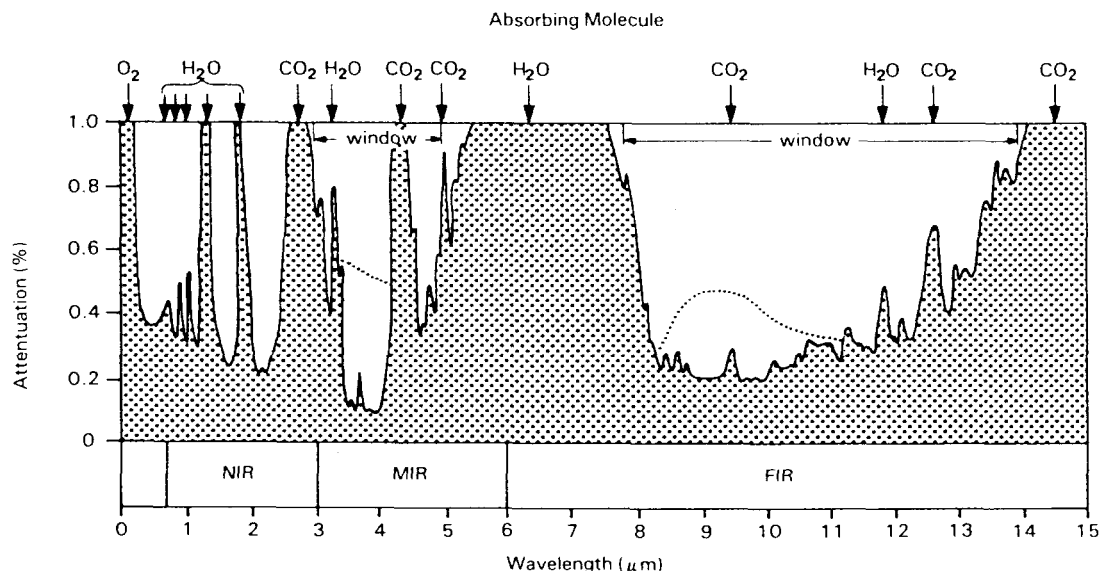


FIG. 4—ABSORPTION OF INFRA-RED RADIATION OVER A 2000 M PATH CLOSE TO THE SEA SURFACE, INDICATING THE ABSORBING MOLECULES, THE MIR WINDOW (3-5 μm) AND THE FIR WINDOW (8-14 μm). THE DOTTED LINE INDICATES THE ADDITIONAL LOSS PRODUCED BY SCATTERING EVEN IN CONDITIONS OF GOOD VISIBILITY

Absorption by atmospheric molecules is a highly wavelength-dependent phenomenon which occurs at wavelengths corresponding to the resonant frequencies of molecular vibrations. In the IR region these frequencies correspond to particular modes of vibration experienced by molecules with three atoms such as water (H_2O) and carbon dioxide (CO_2). In the upper atmosphere ozone (O_3) also contributes. The principal constituents of the atmosphere, nitrogen (N_2) and oxygen (O_2), with their high degree of symmetry, do not contribute to absorption in the IR region although oxygen does absorb some visible radiation. The absorption is shown in FIG. 4. The selective absorption of the resonant wavelengths leaves parts of the spectrum which are not, or are only slightly, absorbed. These regions are termed Transmission Windows as these wavelengths are transmitted through the atmosphere with little absorption. There is a window for visible radiation which extends into the NIR (0.4 to $1.3 \mu\text{m}$); other windows occur between 1.4 and $1.8 \mu\text{m}$ and 2.0 to $2.5 \mu\text{m}$ in the NIR but for the detection of ships the important windows are the wider ones spanning 3.2 to $4.8 \mu\text{m}$ in the MIR and 8 to $14 \mu\text{m}$ in the FIR. Absorption outside these transmission windows is so great that detection is effectively confined to the windows.^{3, 4}

The second mechanism, scattering by particles, is also a resonant phenomenon where the scatterers are comparable in size to the radiation wavelength. However, its effects are not as dramatically wavelength-dependent as the absorption mechanism. The degree of scattering depends upon the area of the scatterers and a factor, k , which is a function of the ratio of the radius of the scatterer to the radiation wavelength, λ . The scattering coefficient is $r\pi Nk$ where N is the concentration of particles of radius per unit volume. The value of k is shown as a function of r/λ in FIG. 5. The function is common to all scattering of electromagnetic radiation. Where the solid scattering particles are much larger than the wavelength of the radiation then k is equal to two and the amount of attenuation is solely that expected by interposing material of total area $r^2\pi N$ between the source and any receiver of the radiation. As the particle radius is reduced to a size closer to that of the wavelength the value fluctuates, attenuation reaching a maximum when $r/\lambda = 0.8$. Particles smaller than λ have a decreasing effect, producing little scattering and little attenuation. From this it is evident that particles of, say, $2 \mu\text{m}$ diameter will cause high attenuation of NIR but the FIR will be largely unaffected.

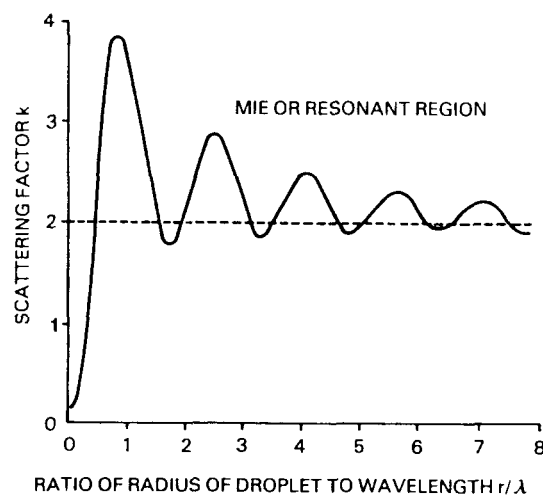


FIG. 5—RELATION OF THE SCATTERING FUNCTION k WITH RELATIVE SIZE OF SCATTERING PARTICLE TO WAVELENGTH

Although attenuation by atmospheric absorption varies little from place to place (especially where the marine environment is concerned, with its high humidity), the attenuation by scattering depends on the nature of the scattering particles present in the atmosphere. These are referred to as the marine aerosol. Over open ocean the marine aerosol comprises water droplets and a relatively stable distribution of small solid particles. The water droplets vary in size from the invisible droplets of haze to large rain drops and depend on local climatic conditions. Although the haze droplets cannot be seen individually their combined effect is to reduce visibility in the optical and IR regions

of the spectrum.

The solids in the aerosol are dust of continental origin and small sea salt particles. The larger (and thus heavier) dust particles descend most rapidly or are prone to other removal processes, coagulation and 'rain out' (in which they become entrapped in rain drops). Only the finest solid particles remain to contribute to the open ocean marine aerosol. The sea salt particles also present are larger and, whilst they do not persist as long, they are constantly being replenished locally in all but the lowest wind speeds and sea states. The bursting of bubbles produced by wind activated wave action ejects small airborne jet droplets which form salt platelets and particles. Because salt is highly hygroscopic the salt component of the aerosol has a size distribution which varies dramatically with humidity. Observations show that, in the humidity levels usually experienced at sea, the particles in the marine aerosol are two to three times greater than they would be if there were very low humidity.

The marine aerosol is a dynamic system with particles continually being generated and removed from the atmosphere. Like ocean waves, the aerosol is affected by both local conditions and by remote conditions at earlier times. High winds, for instance, can increase the number of salt particles thrown into the atmosphere. These are carried to high altitudes and other regions by the winds before they fall back to the ocean.⁵

A general model of the marine aerosol can be described as comprising three superimposed 'log normal', or Zold, distributions (which appear to follow the Gaussian distribution when plotted on log-log graph paper). Particles below 10 nm are not really significant. The largest concentration is of very small particles from the continental aerosol which, because they are so small, persist for long times. They are a maximum concentration at about 30 nm and fall rapidly in concentration as their radius increases to about

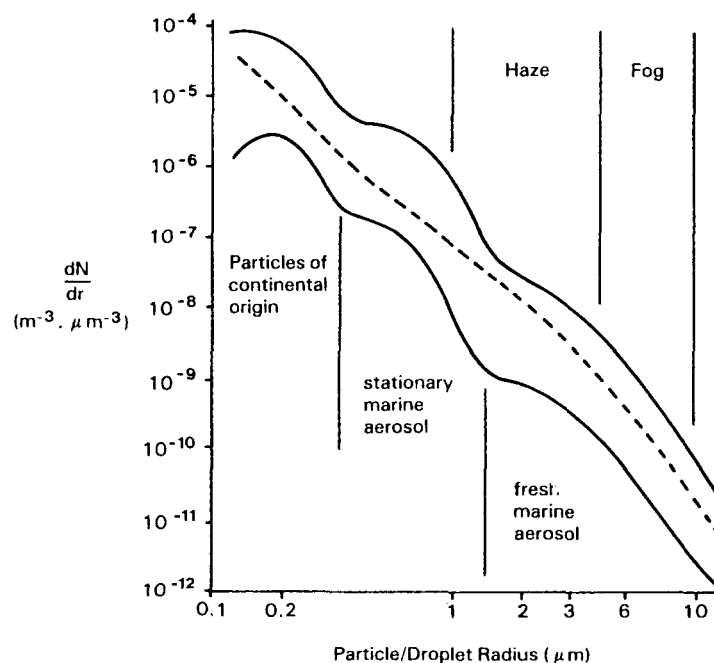


FIG. 6—THE MARINE AEROSOL, SHOWING THE RANGE OF OBSERVED PARTICLE SIZES IRRESPECTIVE OF HUMIDITY OR WIND SPEED. THE BROKEN LINE SHOWS A SEMI-EMPIRICAL RELATIONSHIP OFTEN USED FOR ATTENUATION PREDICTION

300 nm when the 'stationary marine aerosol' becomes dominant. These salt particles, up to about $3 \mu\text{m}$ radius are sufficiently small to persist long enough to form a general background which is largely independent of local conditions. Solid particles larger than this occur in much smaller concentrations and rarely exceed $10 \mu\text{m}$ radius. These rapidly fall back into the sea and are referred to as the fresh marine aerosol. These three contributory distributions all merge in practice and cannot be easily distinguished. FIG. 6 shows the range of concentrations observed and a general distribution curve, often used for transmission prediction, which averages the observations for a large number of humidity and wind conditions.

If the humidity of the air rises to 100%, for instance as warm, moist air cools, then liquid droplets form. Particles in the aerosol, whose diameter is increased many times as the humidity approaches saturation, form nucleation points for the condensation resulting in a haze comprising droplets from $1 \mu\text{m}$ to $5 \mu\text{m}$ diameter. Greater amounts of water condensing will produce the larger droplets of fog. The conditions for fog production are finally balanced and modest changes in temperature can readily disperse fog.

It will be seen that haze and light fog have droplet sizes greater than visible wavelengths and comparable to NIR wavelengths so these wavelengths will be highly attenuated by scattering. MIR and FIR will penetrate haze with the larger wavelength FIR having a capability in light fog. The denser fogs and mists, which are formed when large quantities of water condense, have drop sizes of $10 \mu\text{m}$ to $100 \mu\text{m}$ which very strongly absorb even FIR radiation. As a consequence, IR detection does not represent an all weather capability, although IR detection can operate in some conditions where visible detection cannot be used.

As with visible radiation, IR radiation can penetrate rain to limited extent. The conditions in rain clouds are similar to those in a dense fog, and water droplets fall downwards coalescing to form larger droplets which fall as drizzle or rain.⁶

Scattering can be calculated using classical geometric optics, as the drops are very much larger than the MIR or FIR wavelengths. In general the drop size can be related to the rainfall rate. The Marshall-Palmer distribution, which shows good agreement for rain generated in clouds above 0°C , is plotted in FIG. 7. The distribution is less well defined for colder cloud systems where precipitation begins as ice or snow or where there are strong convective

currents in the clouds. In the latter case distribution displays a discontinuity termed the n_0 jump.

Thunderstorms, which have very strong updraughts preventing all but the largest drops from falling, produce the largest drops and highest rainfall rates (100 mm. hr^{-1}) but these are localized geographically and in time. Although

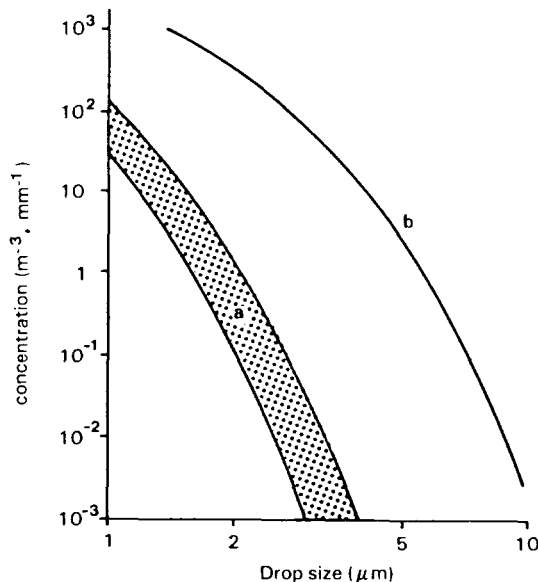


FIG. 7.—DISTRIBUTION OF RAINDROP SIZES ACCORDING TO THE MARSHALL-PALMER FORMULA. CURVE (a) IS THE RANGE OF DROP SIZES IN DRIZZLE (LOWER CONCENTRATIONS) AND LIGHT RAIN. CURVE (b) INDICATES THE SIZES FOR HEAVY THUNDERSTORMS HAVING PRECIPITATION RATES OF UP TO 100 MM/HR

drops in light drizzle are spherical like droplets in haze and fog, drops above about $300\ \mu\text{m}$ are distorted to an oblate spheroidal shape which, above about $1\ \text{mm}$, has a flat base. This can affect the scattering of IR through falling rain which is inhomogeneous where there are large drops. Drops above $10\ \text{mm}$ are unstable. An additional effect of high rainfall rates which affects attenuation is the existence of super-saturation humidity levels up to 3 times greater than those normally experienced. This can increase molecular absorption of the IR radiation.

IR is strongly scattered by snow crystals which are generally larger than $100\ \mu\text{m}$ and have a greater cross-section than the equivalent raindrop of a similar weight. Scattering is affected by diffraction effects which enhance the expected attenuation of the longer wavelengths FIR.

Movement of air and changes in refractive index, such as those caused by convection currents, produce fluctuations in the transmission properties of the atmosphere which can alter the intensity and apparent direction of IR radiation sources. This effect, scintillation, is a major factor limiting the resolution of IR detection.

Effect of Transmission Limitations

The existence of two transmission windows in the absorption characteristics of the atmosphere means that, in practice, there are two signatures to be considered—one in the MIR region of $3\text{--}5\ \mu\text{m}$ and one in the FIR region of $8\text{--}14\ \mu\text{m}$. The black body curves are such that in either window, the hotter the object the greater the emitted radiation. If one were choosing the wavelength to observe a body of a given temperature then the choice would be determined either by the wavelength of a maximum emittance or that of maximum contrast. FIG. 8 plots both of these wavelengths against tempera-

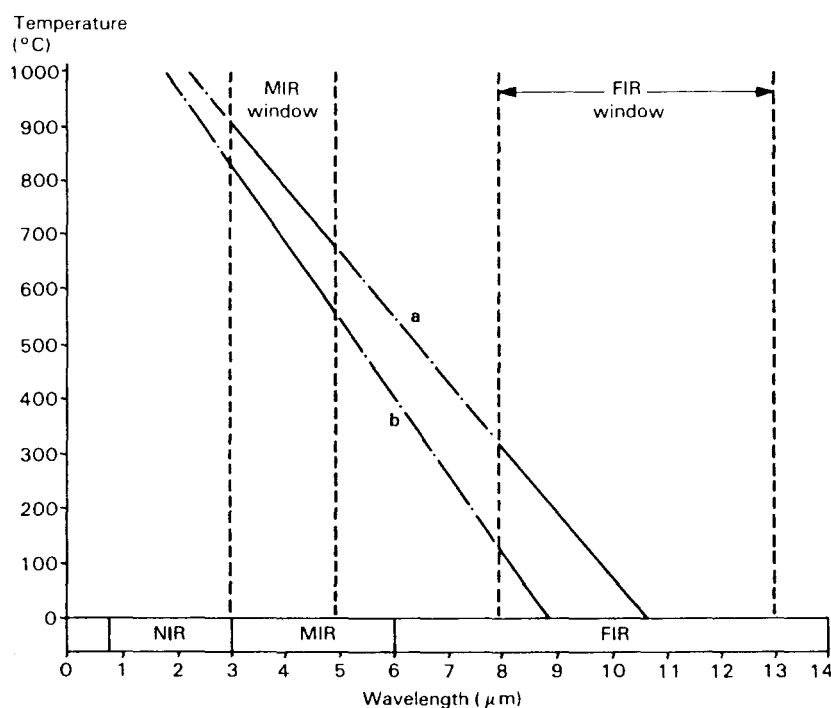


FIG. 8—TEMPERATURE AGAINST WAVELENGTH RELATIONSHIP OF (a) THE MAXIMUM SPECTRAL EMITTANCE, AND (b) THE MAXIMUM RATE OF CHANGE OF SPECTRAL EMITTANCE WITH TEMPERATURE (I.E. CONTRAST)

ture. FIG. 9 is a plot of the total radiant energy emitted by a black body against its temperature. The two lower curves show the amount of this energy emitted between 3 and 5 μm and between 8 and 14 μm . Detectors in the 3–5 μm band have an output against temperature which follows the 3–5 μm curve. Those in the 8–14 μm follow a modified curve as they detect the energy emitted above 11 μm less efficiently. These plots indicate that the 3–5 μm band would be chosen for objects about 600°C. whereas 8–14 μm would be used where cooler objects are concerned. In this latter band the background effects will also be more significant.

The 3–5 μm band is particularly well suited for missile homing heads. Not only are simple detectors available but, by homing on to high temperature parts of the ship, background effects can be ignored. This type of homing head can, however, be decoyed or confused by flares which are also at very high temperatures.

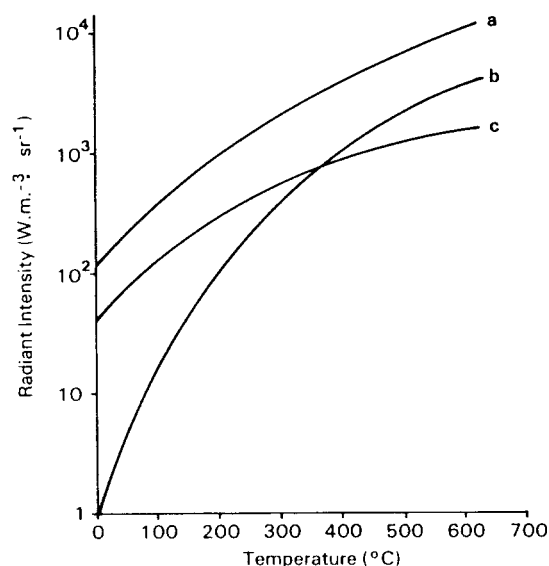


FIG. 9—TEMPERATURE RELATIONSHIP OF RADIANT INTENSITY CURVE. (a) REPRESENTS THE INTEGRAL OF THE BLACK BODY CURVES (THE TOTAL RADIANT ENERGY EMITTED OVER ALL WAVELENGTHS). CURVES (b) AND (c) REPRESENT ONLY THAT ENERGY EMITTED BETWEEN 3–5 μm AND BETWEEN 8–14 μm RESPECTIVELY

The 3–5 μm transmission band can also be used to detect the presence of ships but for identification the detail of the 8–14 μm is needed. Detectors using this band are thus fitted in submarine periscope masts for this purpose and prove particularly useful at night or in poor visibility. Because of the complexity of identifying a ship against a confused background this is most readily performed by human operators. This task is not the same as that performed by 8–14 μm detectors mounted in missiles. To produce the same radiated energy as a ship in the 3–5 μm band a decoy, which has a small radiation area, will burn at a much higher temperature. As it is not possible to match the characteristics of ships and decoys in both detection bands, the addition of the 8–14 μm detector enables the missile to distinguish between decoy and ship. To achieve this, however, the missile designer has to employ special IR windows and increase the complexity of his missile thereby forfeiting warhead space which could otherwise be used for explosives.

In homing, a missile close to the ship is seeking an area of high emittance which may be small compared to the overall size of the ship. On the other hand, in order to identify a ship at longer ranges it is the overall signature of the ship in comparison to its background that is important.

Background Spectrum of Sea and Sky

Ships will be detected against a background IR signature of sea and sky; the ease with which this detection can be achieved will depend on the contrast between the two signatures. The background signatures will comprise contributions from the emission of sea and sky and any radiation reflected from other sources (in practice reflection of the sun's rays from the sea's surface or clouds, or from atmospheric scattering). The amount of energy received by the detector from these sources is strongly influenced by atmospheric attenuation.

The energy emitted from the sun approximates to a black body at 5600°C , with an intensity of 1353 W.m^{-2} falling on the atmosphere. This energy is attenuated by both atmospheric scattering and absorption so that only about two-thirds of this energy reaches the earth's surface. Scattering affects all wavelengths but atmospheric absorption is selective. The spectrum in the lower atmosphere is thus devoid of certain wavelength bands which are strongly absorbed (FIG. 10).

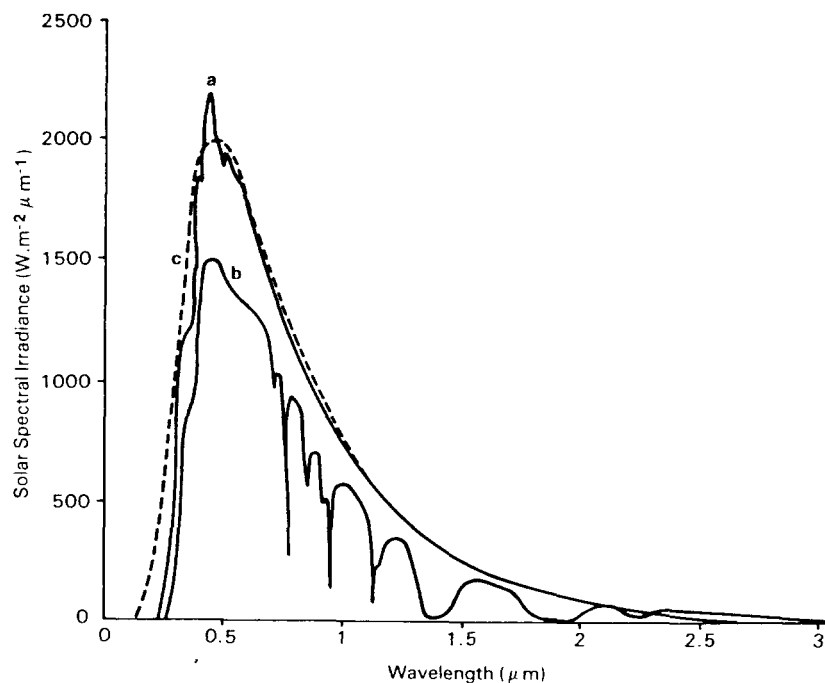


FIG. 10—SOLAR SPECTRAL IRRADIANCE IN THE VISIBLE AND NIR. (a) REPRESENTS THE IRRADIANCE OF THE ATMOSPHERE; (b) REPRESENTS THE IRRADIANCE AT THE EARTH'S SURFACE FOLLOWING ATMOSPHERIC ABSORPTION; AND (c) THE CLOSEST BLACK BODY EQUIVALENT

In clear conditions the sky's spectrum is a combination of scattered sunlight (whose intensity is approximately one millionth of direct sunlight) and radiation from the atmosphere itself, at its ambient temperature (in the region of 20°C). In the bands of interest, $3\text{--}5 \mu\text{m}$ and $8\text{--}14 \mu\text{m}$, atmospheric absorption (and, conversely, emission) is poor. Outside these bands the atmosphere is a good black body emitter whose source is that part of the atmosphere close to the detector. In the transmission windows the source of radiation extends much further—crudely over the distances required to

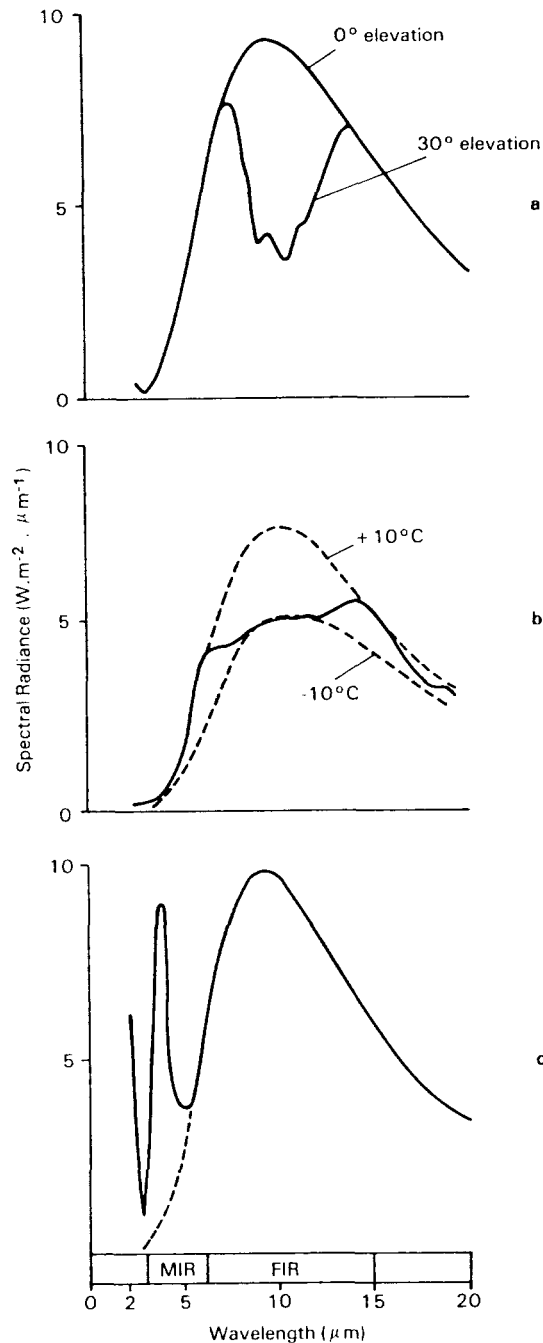


FIG. 11—SPECTRAL RADIANCE OF (a) NIGHT-TIME SKY, (b) UNDERSIDE OF CUMULUS CLOUD, AND (c) SEA SURFACE. BROKEN LINES INDICATE BLACK BODY CURVES

windows, the atmosphere closer to the detector will be most in evidence. FIG. 11(b) demonstrates this in conditions where the cloud is at -10°C and the atmosphere at $+10^{\circ}\text{C}$.

Sea water emits IR radiation from its surface.⁸ The temperature of the few microns closest to the surface determine its effective radiation temperature. Because of the effects of evaporation from the surface, this water close to the surface can be up to one degree cooler than the underlying water. In

significantly attenuate IR radiation by absorption. The effect of this can be seen in FIG. 11(a) which shows the spectral radiance of the night-time sky at zero elevation and at 30° elevation. At low elevation the spectrum emanates from the atmosphere close to the earth's surface. There being a long path length over which emissions can be generated, the spectrum approaches that of a black body. At higher elevations the attenuation of emitted radiation would only be partially absorbed because the path length in the lower, denser atmosphere is relatively short.⁷ Using Kirchoff's relation between absorption and emission we can see that the emission from high elevations will be much less than that of a black body in the region of the transmission windows. The magnitude of the radiance will depend upon the ambient air temperature.

The daytime sky on a clear, cloudless day resembles the night-time sky for the FIR, but in the MIR atmospheric scattering increases the background especially towards the lower end (where the low temperature emissions are, conversely, smaller).

Partial cloud cover can increase the scattered radiation especially in the transmission windows where its absorption is poorest. Full, thick cloud cover, on the other hand, will reduce most of the radiation from the sun so that the emissions of the clouds and atmosphere dominate. In the transmission windows it will be the cloud which will be dominant whereas, outside the

the MIR and FIR regions the emissivity depends little on sea state, however, the emissivity depending strongly on the reflective properties (to which it is related), especially below $7\ \mu\text{m}$. This accounts for the irregular pattern of radiance from sea water shown in FIG. 11(c).

Reflection of IR radiation from the sea's surface provides an important source of background radiation. The amount of radiation from sky or sun which is reflected depends upon the wavelength-dependent refractive index, the sea state and the angle of incidence.

Infra-red Signatures of Ships in the MIR (3–5 μm band)

The IR signature in the MIR transmission window between 3 and 5 μm will be dominated by high temperature objects. These high temperatures are almost solely associated with the prime movers of the propulsion and generation plants. The exhaust gases of diesel engines as they are normally operated in warships are in the range $230\text{--}300^\circ\text{C}$ —whilst gas turbines, now commonly fitted to warships, have even higher exhaust temperatures, up to 500°C at full power. In general the exhaust gas plume and the funnels which carry the exhaust gases are the dominant source of MIR although reflection of sunlight from the superstructure can produce a strong return to certain aspect angles. Deck-parked aircraft and helicopters preparing for take-off (and missile blast screens immediate after missile firing) also produce strong, although transient, emissions on to which missiles may home or which may betray the ship's presence.

Because it is a cavity, an uptake, when viewed from above, appears as an almost perfect black body radiator at the temperature of the exhaust gases.⁸ When viewed from more general threat elevations (up to 20° elevation) the visible area of a vertical uptake is considerably reduced. However, this area will fluctuate as the ship rolls and pitches. Where the exhaust pipe is not vertical (for instance in the Canadian DD 280 Class) the signature will be enhanced at low elevations. Rake or canting of the funnel is not in itself as critical as the shape and orientation of the top of the exhaust pipe. The outside of the funnel can also become hot and emit energy in this region.

The plume of exhaust gases leaving the funnel is a major source of MIR radiation and is discussed further in a later section. As the radiating hot gases and solid combustion products cool rapidly, the signature in the 3–5 μm band is not significant at distances from the funnel which are about twice the funnel diameter (plume dimensions are often quoted in relation to funnel diameter as a convenient means of obtaining non-dimensional relationships).

Apart from the exhaust cavity, the other contributions to the signature are largely independent of the angle of elevation at which it is viewed.

Glint from sunlight can cause problems with detection in the MIR. This glint may be removed by using information available in the very narrow NIR transmission window not normally used in ship detection, as it is useful only for detecting extremely hot sources.

Infra-red Signatures of Ships in the FIR (8–14 μm band)

The very hot sources of radiation will dominate the 8–14 μm band as they do the 3–5 μm band; however, the emission of cooler parts of the ship will there be closer to the intensity of the hot parts. The high contrast of the emissions of these lower temperature areas means that high resolution FIR detectors can reveal a great deal of fine structure which can be used for



FIG. 12—A TYPICAL THERMAL IMAGE OF A MERCHANT SHIP, IN THE 8-14 μM BAND

identification. As can be seen from Figs. 12 and 13 it is possible to detect the warmer parts of the ship's hull surrounding the machinery spaces. Variation of temperature or emissivity, or both, allow many features to be distinguished. The efflux plume can be detected much further from the ship than in the FIR as its gases and efflux solids will remain above ambient temperature for distances of one or two ship lengths from the funnel. The ship's wake can also be detected as it brings to the surface water from lower layers (which are usually cooler) and changes its emissivity by the introduction of air bubbles.

The factors which enable a great deal of information about the ship to be gleaned also lead to a background return which shows a complex structure. This makes the identification of ships difficult and, whilst this can be achieved by a human operator, automatic target recognition using solely 8-14 μm returns is beyond the levels of data processing which can readily be mounted in a missile.

In arctic waters a ship may show up against the background of water or FIR reflected from clouds because its signature has negative contrast—the ship's plating, cooled by the air, being colder than the background.

Propulsion Efflux Plume

The propulsion efflux plume from the funnel is an important source of IR radiation. The mechanism of plume emission and the shape deserves some discussion.

The prediction of plume shape is difficult in the cooler regions far from the exhaust but the shape of the high temperature regions has been described empirically. The shape is largely determined by the cross-wind flowing over, and around, the funnel and superstructure. This cross-wind is the resultant

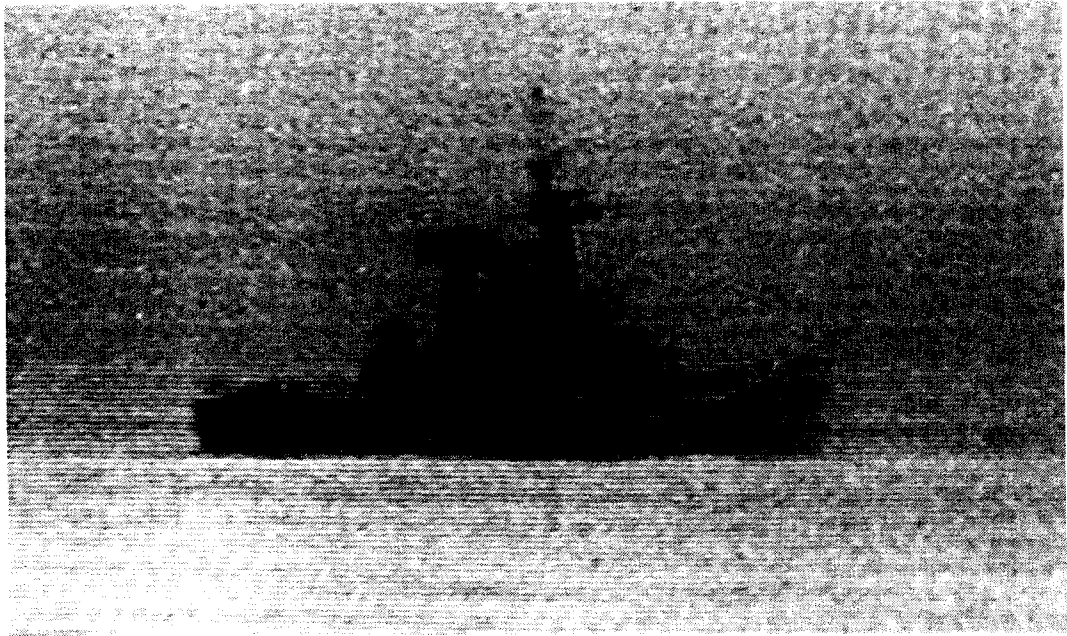


FIG. 13—A TYPICAL THERMAL IMAGE OF A WARSHIP, IN THE 8–14 μM BAND
PHOTOGRAPH BY COURTESY OF BARR & STROUD, LTD.

apparent wind from the combination of wind and ship's motion. Whilst this normally blows from the ahead quarters, a strong wind astern can result in an apparent wind which produces a plume forward of the funnel. The angle between the cross-wind and the ship's heading is termed the yaw angle. The asymmetry of the ship's superstructure and any asymmetry of the funnel will result in a different plume shape as the yaw angle varies. Because both superstructure and funnel are generally longer than they are wide, the plume shape is approximately constant up to about 60° of yaw but apparent winds on the beam or from astern will produce very different shapes. The cross-wind does not flow smoothly over the superstructure. The many bluff surfaces produce turbulence with vortices generated both to windward and leeward of the vertical faces. Even cylinders disrupt the flow and produce turbulence in their lee. The turbulent layers close to the ship give way slowly to the laminar flow regions some distance from it, there being no sharp boundary between them.

The efflux leaving the ship's funnel is projected vertically by its vertical momentum enhanced by the natural buoyancy of hot gases. If the funnel is tall enough, and the vertical velocity high enough, then the plume forms in the laminar region above the ship. If not, the gases are entrained in the turbulent region leading to 'downwash' where they impinge upon the ship's antennas and upper deck equipment. This is undesirable because the efflux contains corrosive products. Heating of the upper deck equipment by the efflux can also enhance its signature in the 8–14 μm band. On the other hand, the rapid mixing which occurs in the turbulent region does cool the plume rapidly and decrease the 3–5 μm signature. There are advantages to designs which release efflux into the top of the turbulent layer (for instance, the USN FFG7 OLIVER HAZARD PERRY Class frigates).

Downwash can be minimized for low yaw angles by streamlining the funnel. The well-defined boundary of a plume in the laminar cross-wind has a radius which increases as it travels downwind. However, it may be difficult to prevent the plume from entering the turbulent region when cross-winds

are close to the beam. This is rarely of consequence, as the downwash is unlikely to reach deck level until it is downwind of the deck edge.

Empirical relationships, based on U.S.N. and R.N. data, which describe the plume shape and temperature are outlined in the Appendix (p. 172). The shape of the plume means that its signature is largely independent of the elevation angle at which it is viewed.

The efflux gases of diesel engines and gas turbines contain two significant sources of IR radiation, carbon dioxide and carbon particles (soot). The solid carbon particles are matt black and radiate as almost perfect black body radiators. The amount of carbon, loosely referred to as smoke, can be measured in a number of ways, one of which is the Bacharach scale. A value of 3.5 on this scale, which represents the limit of visible smoke, would be typical of the amount of soot produced by the correct operation of an advanced gas turbine running above 10% power with the usual R.N. style exhaust arrangement. Although visible smoke would produce a high signature, even a correctly operated engine producing no visible smoke could have a signature with a significant contribution from soot, having an overall emissivity of between 3 and 10% of a black body.

The major source of IR radiation in a plume which has no visible smoke is carbon dioxide. There are two carbon dioxide resonant frequencies at about $4.3 \mu\text{m}$ (FIG. 14). The higher the temperature, the wider these bands; at typical efflux temperatures (above 300°C .) they merge to become a single emission source covering $4.2\text{--}4.8 \mu\text{m}$. This source can be readily detected at short ranges. At longer ranges, however, the emissions in the $4.2\text{--}4.3 \mu\text{m}$ region are strongly absorbed by the cooler carbon dioxide in the atmosphere. This atmospheric carbon dioxide exhibits the narrow twin absorption peaks characteristic of the lower temperature gas.

Carbon dioxide also emits MIR radiation at about $2.8 \mu\text{m}$ but the intensity of this emission is only 10–20% of that at $4.4 \mu\text{m}$ and suffers from greater atmospheric attenuation and greater background interference than the longer wavelengths.

Principles of Signature Reduction and Modification

There are a number of counter-detection techniques which can be applied

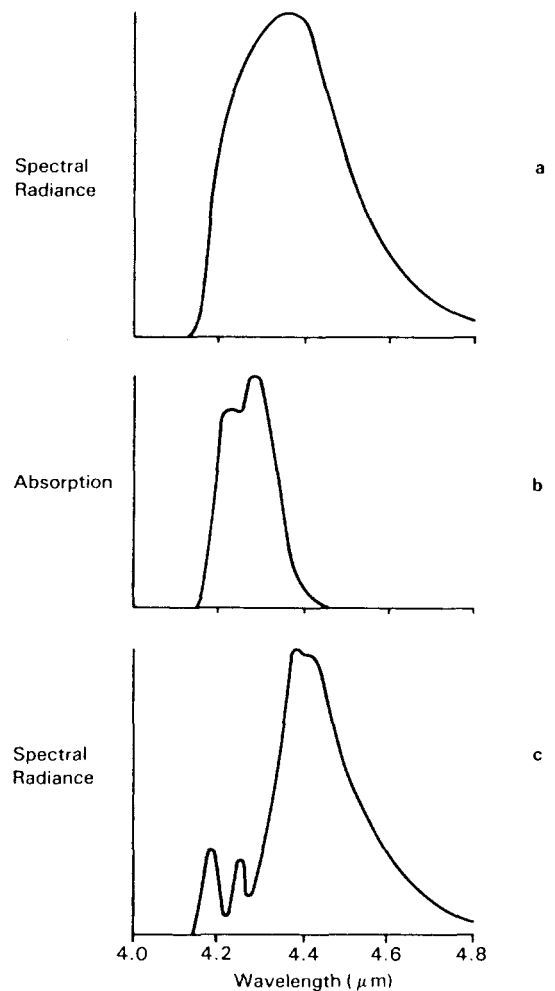


FIG. 14—(a) CARBON DIOXIDE EMISSION SPECTRUM AS OBSERVED CLOSE TO HOT EFFLUX GASES
(b) ABSORPTION SPECTRUM OF AMBIENT ATMOSPHERIC CARBON DIOXIDE
(c) RESULTANT EFFLUX SIGNATURE DETECTED AT LONG RANGE

to all methods of ship detection. They are:

- (a) Reduction in the energy available to the detector.
- (b) Giving the signature the appearance of the background.
- (c) Screening the ship from the detector.
- (d) Provision of a decoy.

For some time these techniques have been applied to visual detection, where they are termed camouflage.⁹ The techniques are not wholly independent and their relationship in IR signatures follows logically. First, it is essential to reduce the radiation of any very hot objects as, without this, the ship cannot merge into the background or hope to deploy an effective decoy. If this cannot be achieved some benefit can be derived from the reduction of the signature in the direction of the greatest threat, principally the lower elevations. If the reduction techniques are successful then it is worthwhile considering the modification of the signature, especially in the 8–14 μm band, to make identification more difficult. Decoys can also be used where the signature has been reduced and is unlikely to dominate.

The object of counter-detection is not to make detection impossible, merely to increase the opposition's difficulties in a game of thrust and counter-thrust. Reducing the signature and merging with the background increases the opposition's false alarm rate. This can be overcome, but only at the cost of more sophisticated and expensive equipment. It also allows more realistic decoys to be used which further reduces the probability of a successful attack by the enemy.

Signature Reduction in the MIR

Signature reduction in the MIR is mainly concerned with the reduction of radiation from hot parts of the ship, principally by temperature reduction.

The hottest potential external surface of the ship, the outside of the uptake, is shrouded by the funnel. Alternatively, its temperature can be reduced by insulation. Signature reduction of the uptake cavity and plume is more difficult. The former requires the cooling of the inner surface of the uptake. The plume can be cooled by entraining large quantities of air in the exhaust trunking (Fig. 15(a)) which introduce between 0.8 and 1.0 times the exhaust gas volume.^{10, 11} This reduces the efflux plume temperature from the

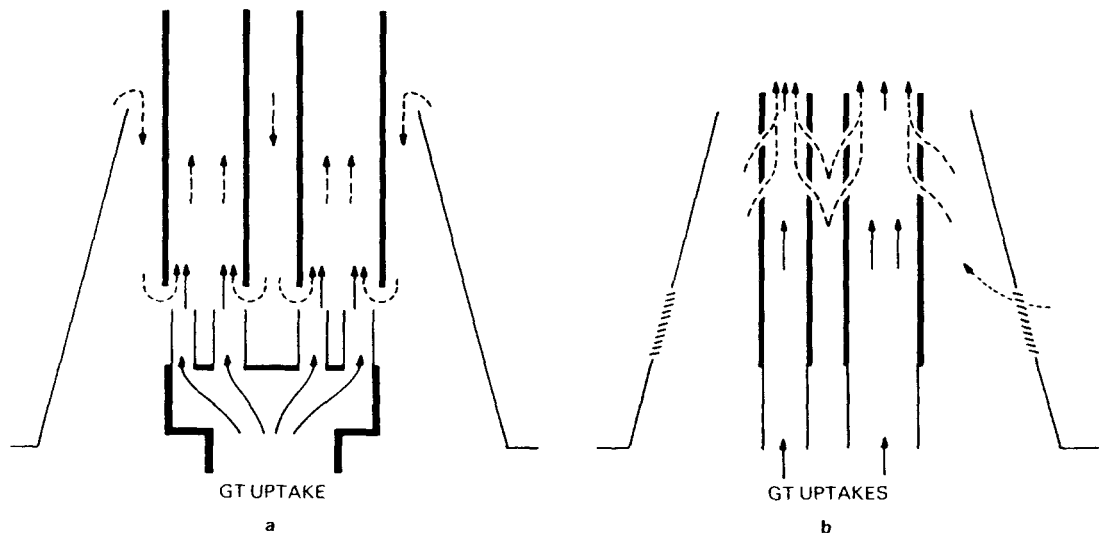


FIG. 15—SCHEMATICS OF AIR ENTRAINMENT WITHIN FUNNELS FOR (a) DILUTION, AND (b) ANNULAR COOLING

normal gas turbine temperatures to temperatures comparable to those of steam boiler exhausts. The disadvantage of air eductors is that, apart from increasing the cost and top weight of the vessel, they may cause difficulties with the exhaust which may then have too low a momentum and buoyancy to pass into the laminar region of air flow above the vessel. For the same reasons the back pressure on the propulsion plant will increase. Waste heat recovery systems (for instance, RACER) will also cool the efflux effectively with the removal of energy. This will also reduce the buoyancy of the efflux (an inevitable concomitant to temperature reduction) and lead to similar problems.

An alternative technique entrains air only close to the walls of funnel. This has the effect of cooling the walls and reducing the apparent cavity temperature, especially at low angles of elevation which receive radiation from the upper parts of the inside of the funnel. This method, termed Bliss Cooling (FIG. 15(b)) introduces a cool annulus of carbon dioxide rich efflux around the plume which absorbs much of the radiation from the hotter core. This technique, like bulk air entrainment, involves large funnels and a topweight penalty. The R.N. 'Cheesegrater' exhausts predate the Bliss coolers and use air blowers thereby avoiding the large volume and weight of funnel which the U.S.N. accepted when they adopted the Bliss coolers. Circulating cooling water within a liner of the funnel will have a similar effect but represents a high topweight penalty and introduces the possibility of condensation and corrosion. Air entrainment techniques can reduce the emitted radiation by two or three orders of magnitude.

Cooling the efflux by water sprays has also been suggested but this would produce severe corrosion if salt water were used. The condensation produced in the plume could enhance the visual signature.

The signature of efflux cavities can also be reduced by the use of screens, especially where the cavity is not vertical. Plates mounted in front of diesel exhausts are a typical example. These must be well clear of the efflux to avoid direct impingement. Although these may remain cool enough to suppress the MIR signature there will probably be a residual FIR signature because the plates will absorb some of the efflux heat. The screens must be positioned to operate even at extreme angles of roll.

Techniques proposed for FIR reduction, such as low emissivity paints and pre-wetting, will also have a use in the MIR region especially as designs are developed with the major MIR sources suppressed.

Signature Reduction in the FIR

Because of the importance of the background signature the methods which should be applied to reducing the signature in the FIR are less clear and must embrace the modification of the signature as well as its reduction. Very hot objects will dominate the FIR signature but it is assumed that these have been suppressed by MIR reduction techniques. Provided the average emission of the ship is not much greater (or smaller) than the average background then further reduction of the signature is less important than the removal of large areas of constant emission which delineate the ship (or parts of it) against an irregular background.

Detection in the FIR is similar in many ways to visual detection. In that case, too, the background against which the ship is seen varies from light sky to dark cloud and can incorporate rapid variations of tint and hue. It is clear that in some cases a very low visual signature (a black ship) may be as easily detected than one with a high signature (a white ship). A compromise is adopted by warships painted grey—light grey for lower latitudes where the light is good and darker grey for higher latitudes. Dazzle painting,

alternate irregular dark and light areas, (which return, on average, about the same amount of light as grey) was attempted to prevent visual detection and identification at long ranges by submarines. Although it is debatable whether this was successful the conditions and scenario for which it was designed was a remarkable analogy of submarine detection with FIR.

It is possible to reduce some of the FIR radiation, if considered necessary, by insulating warm compartments. Low emissivity paints (with values less than 0.5) are still experimental but show promise in reducing and modifying FIR signatures. Of course, low emissivity implies low absorption which reduces the heat absorbed from sunlight but also means that more is reflected and, consequently, they may find more use in locally modifying, rather than reducing, the signature. In such conditions the use of the pre-wetting system can readily match the ship's signature to that of the surrounding water. This also tends to blur the ship's outline and can be considered a screening technique. Pre-wetting cannot be used in arctic waters where icing may occur.

Infra-red Decoys

A flare may be used to present a more attractive target to an IR homing missile. As with most decoys, they can be most effectively deployed if the ship has warning of attack before the homing head has locked on to the ship. The effectiveness of the decoy and the length of warning time are both enhanced in favour of ships where signature reduction and modification techniques have been applied.

IR decoys are often used in conjunction with radar decoys (chaff) as the ship rarely knows which sensor the missile will use in its terminal phase. As with radar decoys, the IR decoys may be used in the distraction mode before the missile is locked on to the ship. This technique provides a number of decoys at long range in the hope that it will lock on to one of these. The other technique, used for close-in defence, is the centroid mode. In this case the IR decoy (and chaff combined with it) is deployed close to the ship. The ship then moves away from the decoy. The missile aims at the emission centre of the combined decoy and ship. The centre of the emission will be closer to the stronger emitter, the decoy. As they part the missile will preferentially home on to the decoy. Some decoys are deployed as a number of flares which light in a sequence each one lighting further from the ship as the previous one burns out. This moves the centroid away from the ship automatically. The flares are usually deployed by rockets or from mortars. The pyrotechnic is generally finely powered aluminium or magnesium mixed with an oxidant such as sodium nitrate. Because of the rapid engagement times involved, a burning time of 30 seconds usually suffices. Flares are supported by parachutes whilst they burn although hot balloons are also used in the distraction mode.

A burning decoy will produce about 3.5 times as much energy in the 3-5 μm band as in the 8-14 μm band. Although this enables them to be distinguished from a ship, the complexity of achieving this task in a missile, coupled with the low ship impact of decoy systems, makes decoys attractive in the protection of ships.

Acknowledgements

I should like to thank Dr J. F. Hardenberg, of the Sea Systems Control-lerate, and Miss E. MacNair for their help in preparing this paper. I should also like to thank Barr & Stroud and Mr J. S. Heslop of ARE(Funtington) for providing the photographs of thermal images of ships.

References

1. Wolfe, W. L., and Zissis, G. J. (ed.): *The infra-red handbook*; Office of Naval Research, Arlington, Va., 1978.
2. Hudson, R. D. jnr.: *Infrared system engineering*; Wiley, 1969.
3. Gebbi, H. A., Harding, W. R., Hilsun, C., Pryce, A. W., and Roberts, V.: Atmospheric transmission in the 1 to 14 micron region; *Proc. Roy. Soc.*, vol. **A206**, 1951, pp. 87-107.
4. McClatchey, R. A., Fenn, R. W., Selby, J. E. A., Volx, F. E., and Garing, J. S.: *Optical properties of the atmosphere*; Air Force Cambridge Research Laboratories, Hansom Field, Ma., 3rd edn., 1972, AFCRL-72-0497.
5. Gatham, S. G.: The effects of meteorology on the marine aerosol and optical and IR propagation; *Proc. AGARD Conference no. 346 on Characteristics of the Lower Atmosphere influencing Radio Waves Propagation, Neuilly-sur-Seine, 1984*, paper no. 7.
6. Pruppacher, M. R., and Klett, J. D.: *Microphysics of clouds and precipitation*; D. Reidal, 1978.
7. Bell, E. E., Eisner, I. L., and Oetjen, R. A.: Spectral radiance of sky and terrain at wavelengths between 1 and 20 microns. Pt. II. Sky measurements; *Journal of the Optical Society of America*, vol. **50**, 1960, pp. 1313-1320.
8. Eisner, I. L., Bell, E. E., Young, J., and Oetjen, R. A.: Spectral radiance of sky and terrain at wavelengths between 1 and 20 microns. Pt. III. Terrain measurements. *Journal of the Optical Society of America*, vol. **52**, 1962, pp. 201-209.
9. Hartcup, G.: *Camouflage*; David & Charles, 1979.
10. Dupuy, P. A.: Combined diesel and LM2500 gas turbine propulsion enhances corvette/frigate missions; *A.S.M.E. Gas Turbine Conference, Amsterdam, 1984*, paper no. 84-GT-195.
11. Bahan, G. J., and McCallum, D.: Stack technology for naval and merchant ships; *Trans. Soc. Naval Architects & Marine Engineers*, vol. **85**, 1977, pp. 324-349.

APPENDIX—SHAPE AND TEMPERATURE DISTRIBUTION WITHIN THE EFFLUX PLUME

On the basis of USN and RN data, the centre-line of a plume in the laminar region can be described empirically in terms of the height y above the funnel top and the distance downwind x , when these are expressed in non-dimensionally as ratio of the funnel exit radius r . The relationship is in terms of the ratio of the exit velocity V_e to the cross-wind velocity V_w and the ratio of the exit temperature T_e to the ambient air temperature T_a (given as absolute values):

$$y = \frac{2k(V_e/V_w)(x/r)^{0.48}[(T_a/T_e)^{5.7} + 0.063]}{2.4 + 0.3(V_e/V_w)^{0.5}}$$

where $k = 8.6$ for single funnels
and $= 6.6$ for multiple funnels

The temperature of the mid-point of the plume, T_m , can be calculated for any distance, s , along the plume path by:

$$T_m - T_a = 5.86 (V_e/V_w)^{0.25} [(2r/s)^{1.44} + 0.017] [(T_a/T_e)^{4.5} + 0.20] (T_e - T_a)$$

The radius of the plume at a distance y from the stack is:

$$r_y = r + [0.3 + 2.4(V_w/V_e) - (1/2F^2)]y$$

where

$$F^2 = (V_e^2/gr)(T_e/(T_e - T_a))$$

and the temperature at a radius r from the centre line by:

$$T_r - T_a = [1 - (r/r_y)^{1.5}] (T_m - T_a)$$

These empirical formulae give a useful indication of the extent of the plume and temperatures in the plume.